TITLE: An Experimental Examination of the Relationship between Chemiluminescent Light Emissions and Heat-release Rate Under Non-Adiabatic Conditions

# An Experimental Examination of the Relationship between Chemiluminescent Light Emissions and Heat-release Rate Under Non-Adiabatic Conditions

L. C. Haber, U. Vandsburger, W.R. Saunders and V. K. Khanna
Reacting Flows Laboratory, Department of Mechanical Engineering
Virginia Tech, Blacksburg VA 24061-0328, USA

## ABSTRACT

Combustion instability research has matured over the last decade and with it the need for more detailed diagnostics has increased. One main gap in the diagnostics is the ability to obtain a reliable quantitative measure of unsteady heat-release rate. In an effort to move in this direction using chemiluminescence as the measured quantity, this paper examines the formation of chemiluminescent light in premixed flames under non-adiabatic conditions. The main chemiluminescent emitters considered in the study are $OH^*$ and $CH^*$. Experimental results for two types of burners are reported, a laminar Bunsen burner with co-flow and a ceramic honeycomb flat flame burner. The study shows that although the chemiluminescence observed in the two burners behaves very differently with respect to changes in experimental variables, the variation can be fully understood. $OH^*$ chemiluminescence is found to be a good indicator of heat-release in both burners, whereas $CH^*$ chemiluminescence is shown to be insensitive to some changes in heat-release rate. Based on the experimental results, the notion that chemiluminescence yield behaves linearly with flow-rate cannot be universally supported. The non-linear variation observed is shown to correspond to an equally non-linear variation of heat-release with flow-rate. The results of the study thus have important ramifications for the interpretation of chemiluminescence measurements in dynamic combustion environments.

## 1 INTRODUCTION

To truly understand the nature of combustion instabilities the ability to measure the influence of acoustic velocity and pressure perturbations on the flame heat-release rate is indispensable. The heat-release measurement capability is also important in the development of models that predict combustion instabilities. Chemiluminescence measurements have often been made to obtain some qualitative indication of the nature of the above described interaction (Samaniego et al., 1993). Quantitative heat-release rate deductions from chemiluminescence measurements have also been made but on a purely empirical basis, assuming a relationship between heat-release rate and chemiluminescence without direct verification (Langhorne, 1988).

To develop confidence in chemiluminescence as a reliable measure of heat-release rate, the relationship between the two quantities must be fully understood. Previous studies (Price et al., 1968) have not analyzed the connection between chemiluminescence and heat-release in great detail because knowledge of the reaction mechanism was very limited. The work presented here uses a detail analysis of experimental results on two very different burners to help develop the desired level of understanding of the relationship between chemiluminescence and heat-release. The study also has included a large modeling effort (Haber et al., 2000) to help provide a foundation for the analysis results presented below.

The understanding of the relationship between chemiluminescence and heat-release relies heavily on a final complete knowledge of the formation paths of chemiluminescent species. The formation chemistry of chemiluminescent species has received some recent attention (Devriendt and Peeters, 1997) but is still not fully understood. In the case of $OH^*$ the currently accepted mechanism was proposed by Krishnamahari and Broida (1961) and has only been verified indirectly by Porter et al. (1967), by Becker et al. (1977) and by Dandy and Vosen (1992) .

The present study considers $OH^*$ and $CH^*$ as the main chemiluminescent species of interest. $CO_2^*$ has been studied as another possible indicator of heat-release rate (Samaniego et al., 1995) but will not be discussed in this paper. $OH^*$ and $CH^*$ are the major chemiluminescence emitters in lean hydrocarbon flames, apart from the $CO_2^*$ emission continuum.

*Paper presented at the RTO AVT Symposium on "Active Control Technology for Enhanced Performance Operational Capabilities of Military Aircraft, Land Vehicles and Sea Vehicles", held in Braunschweig, Germany, 8-11 May 2000, and published in RTO MP-051.*

The fuel used in both present burner studies is methane. Methane was chosen not only for its relatively well known reaction mechanism but also because methane forms a large percentage of natural gas, which is used in most modern lean premixed gas turbine combustors. The use of methane gas allows conclusions drawn from the present study with respect to heat-release relationships to be more easily applied to the gas turbine combustor environment. The present report, however, does not include the study of a turbulent type flame. Since however, the chemical kinetic path of methane reaction remains the same in any combustion system, it is expected that at least qualitatively correct deductions about chemiluminescence measurement in gas turbine combustors can be made.

The experimental setup used to perform measurements in each of the burners is discussed in Section 2. Experimental results obtained from these burners are shown in Section 3. Analysis of the results with respect to heat-release rate and chemiluminescence formation paths is presented in Section 4. Conclusions and ongoing research are given in Section 5.

## 2 EXPERIMENTAL SETUP

### Bunsen burner

The Bunsen burner used in the present study consists of a 12 mm stainless steel tube that is mounted concentrically into a long quartz chimney. The shroud around the stainless steel burner is required to protect the Bunsen burner flame from drafts. To keep the flame from extinguishing inside the quartz chimney, an annular co-flow of air is added. The co-flow is kept constant for all experiments. To assure flows of relatively low turbulence fine screens are mounted upstream in the main combustion flow as well as in the annular co-flow.

The Bunsen burner flame is such that very lean equivalence ratios could not be tested. The experiments cover a range of equivalence ratios from 0.75 to 1.1. The rich stoichiometries tested serve the purpose of elucidating chemiluminescence formation paths. Flow-rates studied cover the range of air-flow from 55 cc/sec to 75 cc/sec.

### Honeycomb burner

The ceramic honeycomb burner consists of a ceramic matrix of small, 1.12 mm, square channels, that is mounted to the top of a 4 inch to 3 inch carbon steel bell-reducer. The bell reducer is used to thin the boundary layer and generate a flatter velocity profile on input to the honeycomb. The flame obtained by lighting mixture flowing through the ceramic honeycomb is essentially flat. A quartz chimney again protects the flame from drafts. Co-flow is not needed in the honeycomb burner to aid in flame stabilization.

The honeycomb burner in contrast to the Bunsen burner allows the study of very lean mixtures. The experimental study reported in the present paper varies the equivalence ratio between 0.6 and 1.1. The flow-rates studied for the honeycomb burner also have a wider range than that studied for the Bunsen burner. The flow-rates varied from an air-flow of 130 cc/sec to an air-flow of 270 cc/sec.

### Optical system

To collect the chemiluminescence, a two-lens optical system coupled to a fiber-optic cable is used. Each of the lenses has a focal length of 1 inch and is made of fused silica for good ultraviolet light transmission. The fiber-optic cable as well is made of fused silica. The fiber-optic cable used for the Bunsen burner measurements has a diameter of $200\mu m$ while the fiber-optic cable used for the honeycomb burner measurements has a diameter of $1000\mu m$. The lens system in each case was set up to collect chemiluminescence evenly across the entire area of the burner, i.e. the intensity measurement is truly a measure of the total chemiluminescence emitted by the flame.

The fiber-optic cable transmits the collected light to a 0.5 m Ebert monochrometer, where the light is filtered by wavelength. $OH^*$ measurements were performed at 308 nm and $CH^*$ measurements were performed at 431 nm. In order to allow relative comparisons between $OH^*$ and $CH^*$, each of the voltage measurements was corrected not only for the wavelength dependent losses in the optical train but also for the spectral shapes of the radiation emitted by $OH^*$ and $CH^*$. Several complete spectra at various experimental conditions on both burners were measured to calculate an integrating scale factor to be used in correcting the single wavelength voltage measurement for the fact that the voltage only represents a certain part of the total energy radiation by the transitions of a certain type of molecule. Upon correction of the voltage in this manner, a measure of the true chemiluminescence yield from the entire flame is obtained. Units for the corrected chemiluminescence are given as (cV-A), which stands for corrected volt - Angstroms.

## 3 EXPERIMENTAL RESULTS

### Bunsen burner

The results for the $OH^*$ chemiluminescence yield variation with equivalence ratio for all flow-rates studied are shown in Figure 1. The maximum for the chemiluminescence is located near stoichiometric mixture conditions. The decrease in chemiluminescence on the rich side is somewhat less steep than on the lean side. The dependence of $OH^*$ on equivalence ratio resembles that of laminar flame-speed on equivalence ratio. The shape of the curve does not appear to change significantly between flow-rates. Furthermore, each of the curves seems to be equally spaced at each equivalence ratio, suggesting a linear dependence of chemiluminescence on air-flow rate. Scaling relationships for Bunsen burner chemiluminescence are examined further in Section 4.

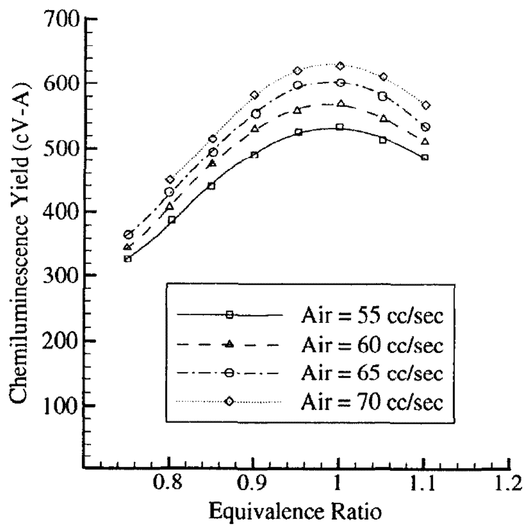


**FIGURE 1:** $OH^*$ chemiluminescence yield as a function of equivalence ratio for the Bunsen burner flame

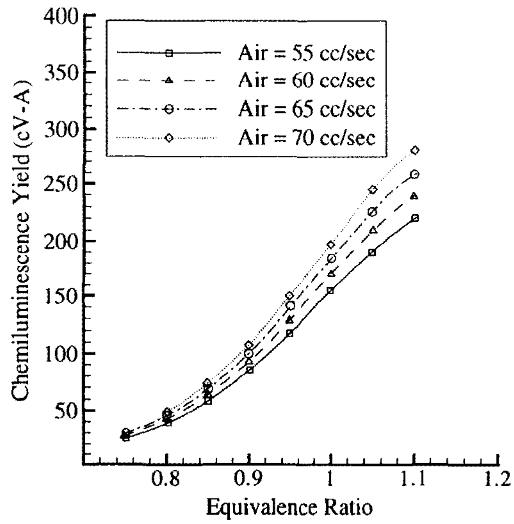


**FIGURE 2:** $CH^*$ chemiluminescence yield as a function of equivalence ratio for the Bunsen burner flame

The $CH^*$ chemiluminescence variation with equivalence ratio for all flow–rates studied is shown in Figure 2. $CH^*$ behaves very differently from $OH^*$. The peak for $CH^*$ chemiluminescence lies on the rich side, beyond the range of the experimental conditions studied. As stoichiometric conditions are approached from the lean side, a near exponential dependence on equivalence ratio is found. $CH^*$ chemiluminescence increases six-fold over the equivalence ratio range studied. $OH^*$ chemiluminescence in contrast only exhibits an increase of 85%. The scaling relationship with flow–rate is not immediately clear upon examining Figure 2. If the dependence on flow–rate is linear for each equivalence ratio, the proportionality factor changes drastically in the equivalence ratio range studied.

### Honeycomb burner

The honeycomb burner results are shown in Figure 3 and Figure 4. At an air flow–rate of 270 cc/sec, the experiment was limited to equivalence ratios below 0.925 due to the onset of a combustion instability. The variation of $OH^*$ chemiluminescence yield with equivalence ratio for several air flow–rates is shown in Figure 3. Peak $OH^*$ chemiluminescence for the honeycomb burner is observed near an equivalence ratio of 0.90. As the air flow–rate is increased chemiluminescent emission increases and the shape of the curve stays approximately the same. The honeycomb burner results differ significantly from those found for the Bunsen burner. The Bunsen burner $OH^*$ chemiluminescence exhibited the peak yield near an equivalence ratio of 1.0. Full analysis of the results is presented in Section 4, but the fact that flame area for the honeycomb burner remains constant for all experimental conditions is bound to contribute significantly to the differences observed between the two burners.

The variation of $CH^*$ chemiluminescence yield with equivalence ratio for several air flow–rates is shown in Figure 4. Peak $CH^*$ chemiluminescence for the honeycomb burner is observed near an equivalence ratio of 1.00. The decline of $CH^*$ emission for leaner mixtures is much steeper than the decline of emission for richer mixtures. The emission of $CH^*$ chemiluminescence almost appears to be leveling off for equivalence ratios above 1.0. As the air flow–rate is increased chemiluminescent emission increases and the shape of the curve stays approximately the same with the possible exception of the data for the high air flow–rate of 270 cc/sec. The large increase in chemiluminescence may be due to the relatively large increase in flow–rate. The dependence on flow–rate, as was seen for the Bunsen burner is very equivalence ratio dependent. Whereas in the honeycomb burner the $CH^*$ chemiluminescence yield for all flow–rates appears almost equal at low equivalence ratios, a drastic dependence on flow–rate is seen at higher equivalence ratios.

## 4 ANALYSIS AND DISCUSSION

The experimental results presented in Section 3 demonstrate how chemiluminescence measurements are particular to a specific burner and chemiluminescence type. The aim of the present paper is to elucidate the observed chemiluminescence trends with experimental variables in terms of associ-

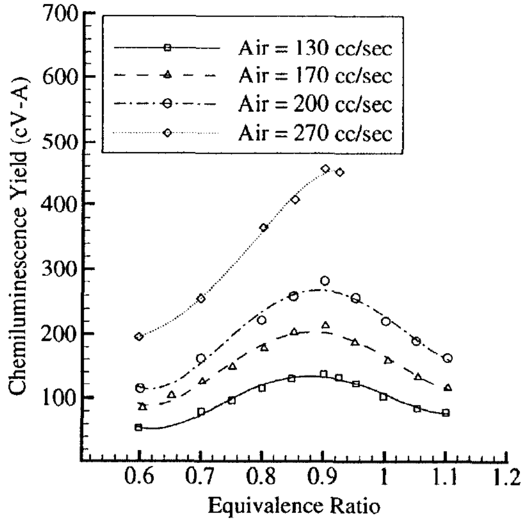


**FIGURE 3:** OH* chemiluminescence yield as a function of equivalence ratio for the flat flame honeycomb burner

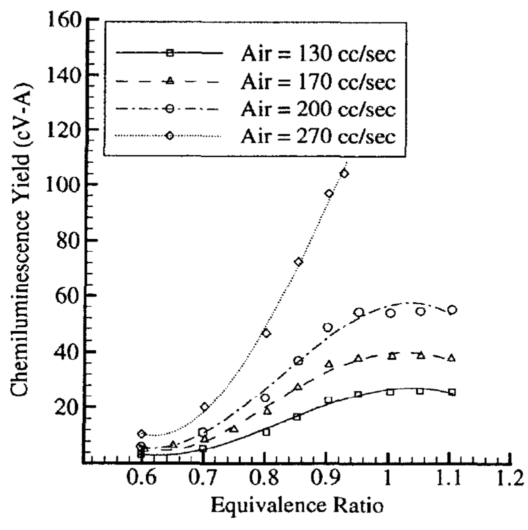


**FIGURE 4:** CH* chemiluminescence yield as a function of equivalence ratio for the flat flame honeycomb burner

ated variations in heat–release. To accomplish the analysis goal, the chemical kinetics of the chemiluminescent species and the combustion as well as other physical processes occurring in each of the burners are studied in detail. In the course of the analysis, each of the chemiluminescent species will be evaluated as a potential indicator of heat–release.

The discussion of the analysis results will benefit greatly from an introduction to the formation paths of the two types of chemiluminescence considered. The introduction focuses on chemiluminescence formation in methane combustion, although some of the conclusions are applicable for higher hydrocarbon combustion as well. A lot of the information pertaining to reactions involving precursors of chemiluminescence species was obtained by examining GRIMECH 3.0 (1999) .

## Chemiluminescence formation paths

In combustion environments CH* is predominately formed from $C_2H$ and atomic oxygen. The reaction was studied in detail by Devriendt and Peeters (1997) who found the reaction to have a low activation energy. The concentration of the precursor $C_2H$ depends greatly on the concentration of $C_2H_2$. $C_2H$ forming reactions have both comparatively high and low activation energies, depending on the other species participating in the reaction. The formation paths of $C_2H$ and CH* are illustrated in Figure 5. $C_2H_2$ forming reactions are not high activation energy reactions but are clearly very sensitive to the concentration of carbon radicals. The large variation of CH* with equivalence ratio is a good indicator of this fact.

OH*has long been thought to be the product of a reaction between CH and molecular oxygen, but recently Haber et al.(2000) have suggested that OH* is formed by a reaction between the formyl radical (HCO) and atomic oxygen. The reaction rate constant used, similar to CH*, has a low activation energy. The formyl radical (HCO), precursor of OH*, is an important intermediate species in methane combustion because HCO–consuming reactions are generally very exothermic and contribute significantly to flame heat–release. HCO is formed primarily from $CH_2O$. HCO–forming reactions generally have no or very low activation energies as illustrated in the reaction diagram shown in Figure 5. HCO consumption reactions however exhibit a variety of activation energies.

## Analysis of experimental results

Researchers starting with Clark (1958) have found that all types of chemiluminescence commonly measured including OH*, CH* and $C_2^*$ vary linearly with Reynolds number, i.e. flow–rate. The slope of the lines varied with equivalence ratio for each of the chemiluminescence types. If one assumes that the heat of reaction per unit mass of fuel is constant with flow–rate, then the linear relationship found indicates that chemiluminescence is a good indicator of heat–release rate. Indeed, normalizing the CH* chemi-

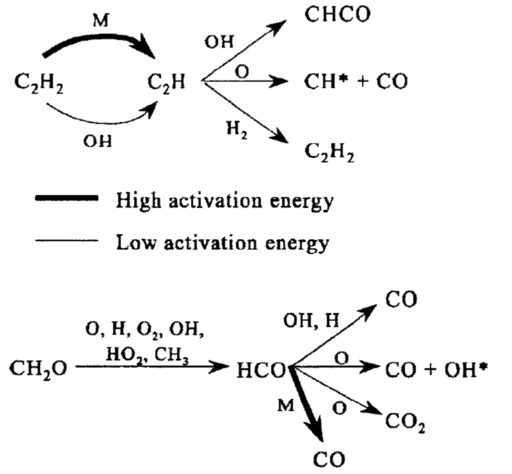


**FIGURE 5:** Reaction diagram for the production of CH* and OH* chemiluminescence

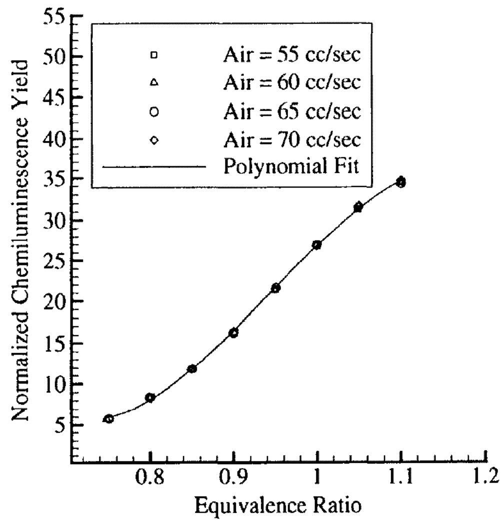


**FIGURE 6:** Normalized CH* chemiluminescence yield as a function of equivalence ratio for the Bunsen burner

luminescence results for the Bunsen burner by dividing by the fuel flow–rate yields a single curve, that is a function of equivalence ratio only as shown in Figure 6. As a result one may want to write a functional relationship of the form $I_{CH^*} = F(\phi\ , \dot{m}_{fuel}\ \Delta\text{HR})$. However, the heat–release rate calculated by multiplying the the heat of reaction by the fuel flow rate does not account for the fact that not all heat liberated by chemical reaction contributes to the enthalpy change in the gas. Some heat is lost to the surroundings by radiation and conduction.

The sensible enthalpy change, which is related to the total temperature increase across the flame is however the quantity of interest in combustion dynamics research. A time rate of change of the temperature increase of the gases through the flame causes a time rate of change of the gases' acceleration through the flame. The time variation of the acceleration causes the flame to act like an acoustic source and drives the combustion instability. An appropriate indicator of heat–release must be sensitive to changes in the temperature increase of the gases through the flame.

It is thus important to check the sensitivity of the given indicator to changes in the temperature rise through the flame, independent of changes in the total heat liberated and changes in equivalence ratio. The examination of the OH* experimental results for the Bunsen burner is an excellent example of a case where chemiluminescence is not merely a function of the total heat liberated and the equivalence ratio.

As was done for CH* chemiluminescence, OH* Bunsen burner results were normalized with fuel flow–rate. In contrast to CH*, OH* chemiluminescence does not collapse onto a single curve. The OH* chemiluminescence results need to be further normalized by multiplying by the square root of Reynolds number. The resulting curve of normalized OH* chemiluminescence as a function of equivalence ratio is shown in Figure 7. The results mean that the amount of OH* chemiluminescence obtained per unit mass of fuel burned is consistently lower at all equivalence ratios tested when the flow–rate is increased, because the normalization required a multiplication by the square root of Reynolds number.

Several clues help in the interpretation of these results. First, as mentioned, the yield of OH* per unit mass of fuel burned is lower for all equivalence ratios including rich equivalence ratios when the flow–rate is increased. Second, a developing boundary layer scales with the square root of Reynolds number. The first clue shows that mixing phenomena are not responsible for the observed scaling because the admixture of air for rich mixtures would increase the yield of OH* chemiluminescence per unit mass of fuel burned by an effective decrease in the equivalence ratio.

The second clue points to another boundary layer dependent phenomenon, that of heat transfer. Indeed, the fine wire mesh screens are mounted less than 5 inches upstream of the burner lip. The boundary layer does not have time to develop fully by the time the flow reaches the burner lip. The result is that heat transfer from the heated stainless steel tube is enhanced for higher flow–rates. The temperature increase in the incoming mixture in turn produces an increase in the flame temperature. The flame temperature increase is not equal to the increase in the incoming mix-

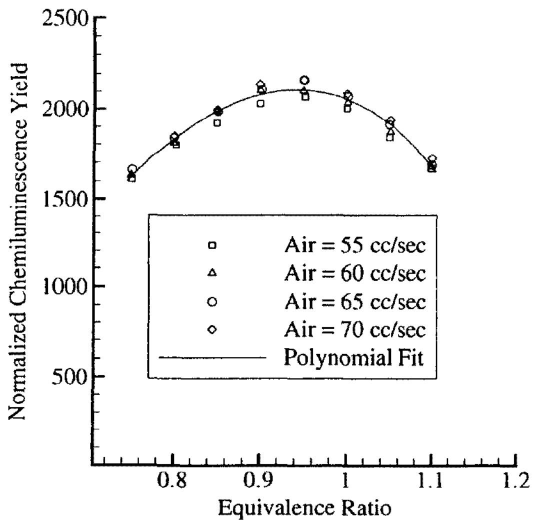


**FIGURE 7:** Normalized OH* chemiluminescence yield as a function of equivalence ratio for the Bunsen burner

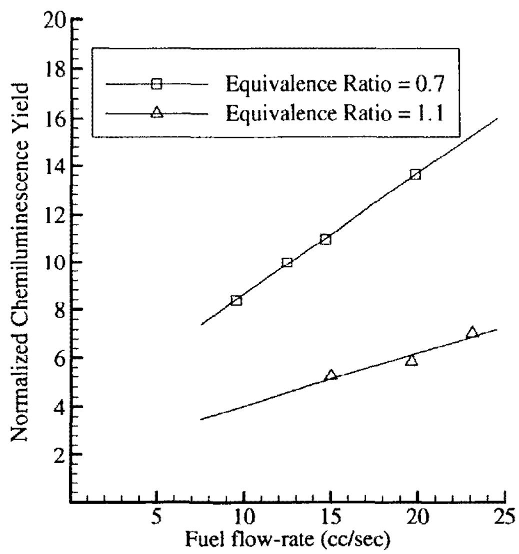


**FIGURE 8:** Normalized OH* chemiluminescence yield as a function of fuel flow-rate for the honeycomb burner

ture temperature due to higher heat–losses by radiation, conduction as well as product dissociation. The increase in temperature within the flame affects OH* formation detrimentally by favoring higher activation energy formyl radical (HCO) consumption reactions (see Figure 5).

Based on the above reasoning, CH* chemiluminescence should have exhibited some sensitivity to the flame temperature change. However, CH* chemiluminescence formation, as discussed above, combines high and low activation energy processes. As a consequence the flame temperature increase enhances some CH* precursor formation reactions and discourages others. The small flame temperature increase therefore is not seen to affect CH* chemiluminescence. Note that the above explanation shows that the decrease in OH* chemiluminescence per unit mass of fuel burned is related to a net decrease in temperature rise across the flame. CH* fails to show the same sensitivity to heat release.

Najm et al. (1998) also found that CH* chemiluminescence was not a good indicator of heat-release rate in methane flame environments of very high curvature, near extinction. The recommended indicator of heat–release rate based on their study is the formyl radical (HCO). As discussed above, the formyl radical is a precursor of OH* which makes OH* an indicator of formyl radical concentration and by inference a good indicator of heat–release rate, even in high flame curvature environments, near extinction.

The quality of OH* chemiluminescence as an indicator of heat–release rate can be verified further by examining the results reported for OH* chemiluminescence on the honeycomb burner. The normalization of the chemiluminescence data by the fuel flow–rate leaves a residual trend with flow-rate. A plot of normalized OH* chemiluminescence versus fuel flow–rate is shown in Figure 8 for equivalence ratios of 0.7 and 1.1. It is seen that for both equivalence ratios the amount of chemiluminescence obtained per unit mass of fuel burned is an increasing function of flow–rate. To validate OH* as an indicator of heat–release rate, as defined above, the dependence of normalized OH* chemiluminescence on flow–rate must be shown to correspond to a relative decrease in heat–losses from the flame.

An analysis of the burning process in the honeycomb burner will help elucidate the chemiluminescence formation process. The flow–rate per unit area of the honeycomb burner is very low when compared to the maximum laminar burning rate. The highest flow–rate studied corresponds to a flow–rate one third of the maximum laminar burning rate. In the honeycomb burner, the flame area is always constant and the reaction rate increases to accommodate increases in flow–rate. Closely tied to increases in reaction rate are increases in the flame temperature.

Reaction rate is an exponential function of temperature. Radiation heat–loss from the flame is a function of the flame temperature raised to the fourth power. For an overall activation temperature of 16000 K$^o$, a base temperature of 1800 K$^o$and a required increase in the reaction rate of 30%, the increase in flame temperature only has to be about 3%. A 3% increase in the flame temperature results only in a 13% increase in radiation heat–loss. The radiation heat–loss is thus relatively lower at a higher burner

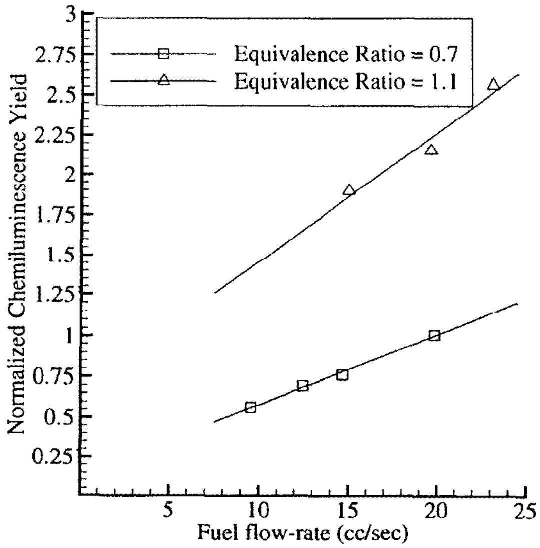


**FIGURE 9:** Normalized CH* chemiluminescence yield as a function of fuel flow–rate for the honeycomb burner

flow–rates. Note also that since the flame temperature is higher, the temperature rise through the flame is higher. The increase in OH* chemiluminescence obtained per unit mass of fuel burned thus corresponds to an increase in the heat–release per unit mass of fuel burned.

As was done for OH* chemiluminescence, CH* chemiluminescence was normalized by dividing by the fuel flow–rate. Figure 9 shows a plot of normalized CH* chemiluminescence as a function of fuel flow–rate for equivalence ratios of 0.7 and 1.1. Again, a residual trend with flow–rate can be detected for both equivalence ratios. The reaction rate increase and associated flame temperature increase appears to affect CH* and OH* chemiluminescence in similar ways. Note that in contrast to the Bunsen burner, the flame temperature increase in the honeycomb burner is not caused by an increase in the temperature of the incoming gas and thus does not exhibit a similar shift towards higher activation energy reactions. The temperature increase in the honeycomb burner is tied to the reaction rate increase necessary to support the higher flow-rate, resulting in an overall increase of the throughput of all reaction paths.

All of the identified scaling relationships and trends have important consequences for the use of chemiluminescence as a dynamic heat–release rate indicator. Assuming the variation in the flow–rate occurs on a much slower time–scale than the reaction rate, the flame will adjust itself to changes in the flow–rate very quickly. Oscillations in flow–rate can then be viewed from a quasi–steady standpoint in terms of the fluctuations in chemiluminescence these oscillations produce. The non–linear scaling relationships and trends reveal that for large oscillations in flow–rate, the oscillations in heat–release rate will show significant non–linear effects. For the honeycomb burner for example, the non–linearity appears to be quadratic in flow rate because normalization by fuel flow–rate leaves an approximately linear residual trend in the same variable.

## 5 CONCLUSIONS

Experimental studies of chemiluminescence were performed for two different types of non-adiabatic burners, measuring OH* and CH* chemiluminescence yield. The experiments covered a wide range of equivalence ratios and flow–rates. The results underlined the fundamental differences between the two chemiluminescent species, especially in terms their variation with equivalence ratio.

An attempt was made to identify all major processes that affect the scaling of chemiluminescence yield with flow–rate. The traditionally accepted view that chemiluminescence yield behaves linearly with fuel flow–rate must be rejected based on the OH* chemiluminescence results in both burners. CH* chemiluminescence on the Bunsen burner was linear with flow–rate but CH* chemiluminescence on the honeycomb burner was found to exhibit similar behaviour to OH* chemiluminescence. The linear relationship with fuel–flow observed on the Bunsen burner confirms the results of the study by Najm et al. (1998) that CH* is not a good indicator of heat–release rate in all flame environments. CH* chemiluminescence fails to capture a decrease in the sensible enthalpy change of the gases through the flame. OH* chemiluminescence does capture the decrease and again further confirms the results of Najm et al. (1998) that the formyl radical and by inference OH* chemiluminescence is a good indicator of heat–release rate.

The results of the analysis, even though strictly valid only in steady combustion environments, have interesting implications for chemiluminescence measurement in dynamic combustion environments. The non–linear scaling of chemiluminescence with flow–rate for a burner may point out important non–linear processes influencing such important combustion instability characteristics as limit cycle amplitude and frequency content.

The present study represents only a small step in the direction of obtaining a quantitative measure of heat–release rate. The conclusions drawn from the experimental results above are currently being verified through a detail combustor modeling effort. The methods used in the experimental study are also going to be applied to more complex flame environments in an effort to achieve the same level of understanding for turbulent flames as for laminar flames. Finally, it is important to mention that experimental studies are currently being conducted on laminar flames in dynamic flow environments.

## ACKNOWLEDGMENTS

The authors would like to acknowledge the support of Mr. Ludwig Haber by a NSF Graduate Fellowship.

## REFERENCES

Becker, K., Kley, D., and Norstrom, R. (1977). $OH^*$ chemiluminescence in hydrocarbon atom flames. *Fourteenth Symposium (International) on Combustion*, pages 405–411.

Clark, T. (1958). Studies of OH, CO, CH and $C_2$ radiation from laminar and turbulent propane-air and ethylene-air flames. *NACA Technical Note 4266.*

Dandy, D. and Vosen, S. (1992). Numerical and experimental studies of hydroxyl radical chemiluminescence in methane-air flames. *Combustion Science and Technology*, 82:131–150.

Devriendt, K. and Peeters, J. (1997). Direct identification of the $CH^*$ chemiluminescence in $C_2H_2$ / O / H atomic flames. *Journal of Physical Chemistry A*, 101:2546–2551.

Haber, L., Vandsburger, U., Saunders, W., and Khanna, V. (2000). An examination of the relationship between chemiluminescent light emissions and heat release rate under non-adiabatic conditions. *Proceedings of the IGTI*, (2000-GT-0121).

Krishnamhari, S.L.N.G. and Broida, H.P. (1961). Effect of molecular oxygen on the emission spectra of atomic oxygen-acetylene flames. *Journal of Chemical Physics*, 34(5):1709–11.

Langhorne, P. (1988). Reheat buzz: An acoustically coupled combustion instability. part 1. experiment. *Journal of Fluid Mechanics*, 193:417–443.

Najm, H., Paul, P., Mueller, C., and Wyckoff, P. (1998). On the adequacy of certain experimental observables as measurements of flame burning rate. *Combustion and Flame*, 113:312–332.

Porter, R., Clark, A., Kaskan, W., and Browne, W. (1967). A study of hydrocarbon flames. *Eleventh Symposium (International) on Combustion*, pages 907–917.

Price, R., Hurle, I., and Sugden, T. (1968). Optical studies of the generation of noise in turbulent flames. *Twelfth Symposium (International) on Combustion*, pages 1093–1102.

Samaniego, J., Egolfopoulos, F., and Bowman, C. (1995). $CO_2^*$ chemiluminescence in premixed flames. *Combustion Science and Technology*, 109:183–203.

Samaniego, J., Yip, B., Poinsot, T., and Candel, S. (1993). Low-frequency combustion instability mechanisms in a side dump combustor. *Combustion and Flame*, 94:363–380.

Smith, P., Golden, D., Frenklach, M., Moriarty, N., Eiteneer, B., Goldenberg, M., Bowman, C., Hanson, R., Song, S., Gardiner, W., Lissianski, V., and Qin, Z. (1999). *http:// www.me.berkeley.edu/gri_mech/.*